Colloid and Polymer Science (2023) 301:801–812
https://doi.org/10.1007/s00396-023-05131-z

ORIGINAL CONTRIBUTION

Linear growth of colloidal dumbbells into three-lobed polymer nanoparticles mediated by a gradient in surface wettability

Gabriel Augusto Alemão Monteiro[1] · **Alexander Wittemann**[1]

Received: 13 February 2023 / Revised: 11 May 2023 / Accepted: 22 May 2023 / Published online: 16 June 2023

Abstract
Anisotropy is a deciding factor in determining the hydrodynamics and self-assembly of colloidal particles. Linking particle morphology to said behaviors promoted the development of strategies to obtain anisotropic particles exhibiting defined shapes and symmetries. Dumbbell-shaped polymer particles made by phase separation during seeded polymerization are prominent examples. Phase separation among monomer and seed particle yields a liquid protrusion of monomer on the seed. This protrusion is then polymerized, becoming solid and yielding a solid spherical lobe. When this process is performed with spherical seeds, two-lobed particles, known as colloidal dumbbells, are obtained. Repeating this process of lobe formation one or more times could pave the way to tailored particle morphologies. Given the higher degree of anisotropy, multi-lobed particles can expand the rich phase behavior already found for dumbbells. We propose a new route in making anisotropic polymer particles by directing phase separation in a linear direction, thus permitting linear growth. Colloidal particles composed of three individual polymer lobes with the potential for site-specific modifications are obtained. Triggering of the phase separation is done complementary to prior efforts in fabricating three-lobed polymer particles based on cross-linked precursor particles. We will show that tailored surface properties of anisotropic seed particles can prove as an effective tool not only to promote the monomer-polymer phase separation, but also to guide it in a linear direction. Such gradients in surface functionalization open perspectives for making polymer colloids on a large scale in whose custom-tailored shapes their phase behavior and superstructure formation are already established.

Keywords Nanoparticles · Anisotropic particles · Polystyrene latex · Seeded polymerization · Colloidal molecules · Dumbbells

Introduction

Anisotropic colloidal particles are known for their unique phase and hydrodynamic behavior [1, 2]. They can be used as rheology modifiers to adjust the decisive physical properties of colloid suspensions, such as the elastic modulus and the yield stress [3]. Their effectiveness is caused by an alignment under shear and is not limited to a mere control of the overall viscosity, as expected when using thickeners. They also add non-Newtonian behaviors to the material such as shear thinning or shear thickening. Adding anisotropic particles can thus help to control shelf stability, ease of application, texture, and processability of a wide variety of products, ranging from food materials, cosmetics, pharmaceutics, or oil-field and construction drilling fluids [4, 5]. Moreover, anisotropic colloidal particles can be expected to become the building blocks of tomorrow's materials [6]. A complex yet defined shape and symmetry can open avenues for programmed assembly into hierarchically organized materials [7]. The latter can exhibit collective properties, which are not yet present in the isolated building blocks. This includes photonic and phononic properties that can emerge from packing the particles into mesoscopic superlattices [8]. The control on particle shape is crucial to achieve precisely controlled superstructures, with long-range order and a minimum number of defects [9].

The enormous potential and the unique behaviors of anisotropic particles led to efforts devoted to developing strategies to either synthesize them directly or to arrange isotropic particles into this kind of morphology [7, 10]. Among

✉ Alexander Wittemann
alexander.wittemann@uni-konstanz.de

[1] Colloid Chemistry, Department of Chemistry, University of Konstanz, Universitaetsstrasse 10, 78464 Constance, Germany

the anisotropic colloids directly obtainable from synthetic routes, dumbbell-shaped polymer particles received considerable attention due to their rich phase behavior and the possibility to obtain them in large quantities using seeded polymerization [11–13]. The possibility of making these anisotropic colloidal particles in large quantities allows their application as building units for hierarchically organized materials, including photonic crystals with specific symmetries at the lattice points. Such superstructures can provide large and robust optical bandgaps over a broad range of visible light paired with birefringence [8]. Considering the synthesis of these colloidal dumbbells, efforts were focused on expanding the understanding of the mechanism, thermodynamics, and kinetics behind their fabrication and on expanding their range of applications [14–16]. These works have pushed the boundaries of what is possible using seeded polymerization and allowed the synthesis of nanoscale dumbbells based on mechanisms reliant either on cross-linking density [17, 18] or surface properties [8, 15].

Regardless of using the cross-linking density or the surface wettability as the driving force to promote the protrusion formation, the synthesis of anisotropic polymer particles is done by using seeded emulsion polymerization [19]. This methodology is based on a phase separation between monomer and polymer within a monomer-swollen seed particle. Given the right conditions, the phase separation leads to the formation of a liquid protrusion attached to the surface of the seed particle. This process is understood to be controlled thermodynamically and reflects the interplay between three free energy components [14]. These are the mixing energy between monomer and polymer; the elastic stress caused by the swelling of the seed particle; and the interfacial tensions between particle, monomer, and the reaction medium. The sum of these three free energy components is defined by synthesis parameters like the monomer-to-polymer ratio and the reaction temperature [16]. The heating that promotes the phase separation also initiates the polymerization and solidification of the liquid protrusion. This polymerization is ensured by the decomposition of a thermal initiator into free radicals inside the protrusion. Once the polymerization is complete, the polymer forms a solid lobe attached to the surface of the seed particle. This lobe grown alongside the seed particle forms a morphology resembling a dimer of interpenetrating spheres [14–17].

In the case of the formation of dumbbell particles, it has been shown that cross-linking of the polymer within the seeds and/or limiting their surface wettability with monomers are effective means to trigger the formation of monomer protrusions, thus guiding seeded polymerizations into an anisotropic dimension [14, 17]. With respect to cross-linking, this concept has been further elaborated. Using dumbbell-shaped particles as seeds with two cross-linked lobes and provoking the phase separation a second time resulted in the formation of particles with three lobes, named trimers or sometimes tripods [20]. Further efforts led to the discovery that a gradient in the cross-linking density between the dumbbell lobes can control the direction in which a second protrusion is formed. This finding paved the way towards linear three-lobed particles, but only on a micrometer scale and exclusively by using cross-linking as a driving force for anisotropic growth [20]. For non-cross-linked particles, however, the influence of a gradient in distinct surface properties between the two lobes is yet to be described.

Aiming to close this gap, this study presents an efficient chemical route to make linear particles composed of three individual nanosized spherical lobes. The three-lobed polymer particles are fabricated by successive seeded polymerizations based on the surface properties of the employed seed particles and on gradations between them. Beyond describing the formation of non-cross-linked polystyrene-based (PS) nanotrimers, the morphological characterization of these particles is shown, including the determination of the angle distribution between the three lobes and the distance between them. This thorough morphological characterization allows for the precise observation of the gradient-mediated direction of anisotropic particle growth.

Materials and methods

Chemicals

The reagents acrylic acid (AA) (99%, Sigma-Aldrich), azobisisobutyronitrile (AIBN) (98%, Sigma-Aldrich), potassium persulfate (KPS) (99%, Sigma-Aldrich), sodium dodecyl sulfate (SDS) (99%, Sigma-Aldrich), and 3-(trimethoxysilyl) propyl methacrylate (MPS) (98%, Sigma-Aldrich) were used as received. Styrene (St) (99%, Merck) was passed through a *tert*-butylcathecol inhibitor remover (Sigma-Aldrich) column immediately before its use in the polymerization reaction. Deionized water (resistivity = 18.2 $M\Omega.cm^{-1}$) taken from a reverse osmosis water purification system (Millipore Direct 8) was used in all experiments. Sucrose (≥ 99.9%, VWR Life Sciences) and dodecane (≥ 99%, Sigma-Aldrich) were used to prepare the density gradients for the differential centrifugal sedimentation experiments.

Syntheses

All polymerizations were carried out in three-neck round-bottom flasks. These were degassed and purged with N_2 before the reagents were added. The flasks were equipped with a precision glass stirrer (KPG), a

polytetrafluoroethylene stirring blade, a reflux condenser, and a silicone septum. All the reactants were added either under N_2 counter-flux or through the septum using syringe needles. The reagent mixtures were further degassed and flushed with N_2 while still at room temperature. The reactions were also conducted under this inert atmosphere. After each reaction, the samples were cooled down to room temperature and filtered through glass wool. The synthesis procedure presented here is an extension of the seeded polymerization methodology to obtain dumbbell-shaped polymer colloids already described in the literature [15], including recent refinements [11, 16].

Synthesis of polystyrene spheres

Spherical PS particles were obtained using batch emulsion polymerization. A 1000-mL reaction vessel was first filled with water (649.20 g, 36.04 mol), SDS (0.9875 g, 3.42 mmol), and styrene (100.62 g, 0.966 mol) before being heated to 80 °C under permanent stirring at 300 rpm. Once the mixture reached the reaction temperature, the radical initiator KPS (0.9494 g, 3.51 mmol) was added dropwise to it as an aqueous solution of 20 mL, a volume taken from the specified mass of water. The reaction vessel was kept at 80 °C under continued agitation for a period of 6 h.

Surface functionalization of PS particles with MPS

For the surface modification of the PS particles, the previously prepared suspension (13.52 wt%, 169.70 g) was diluted with water (188.41 g, 10.46 mol) at 200 rpm inside a 500-mL reaction vessel. A solution of MPS (3.676 g, 14.80 mmol) and AIBN (0.1363 g, 0.83 mmol) in styrene (21.68 g, 0.208 mol) was prepared. The organic solution was added to the suspension through the septum. The whole mixture was kept under agitation for 20 min before a water bath (preheated to 70 °C) was placed underneath, heating the reaction vessel, and thus starting the polymerization and surface modification process. The reaction was continued for a total of 8 h.

Preparation of PS-based dumbbells from the functionalized PS spheres

The surface-modified PS particles were used as seeds in a seeded polymerization process yielding dumbbell-shaped particles. This process was done by first mixing the seed suspension (11.03 wt%, 32.23 g) with water (101.05 g, 5.61 mol) in a 250-mL flask at 200 rpm. Similar to the previous step, a mixture of styrene (3.79 g, 36.4 mmol), AIBN (29.5 mg, 0.180 mmol), and MPS (0.1924 g, 0.78 mmol) was added to the aqueous suspension through the septum via a syringe needle. The reaction mixture was kept under continued agitation for 20 min before being heated to 70 °C by placing a preheated water bath underneath. The reaction took place over a total of 7 h.

Formation of three-lobed PS particles from dumbbells

The formation of trimer particles was conducted in a further seeded polymerization using the dumbbells as seeds. The suspension of dumbbell particles (5.11 wt%, 42.84 g) was first mixed with water (51.38 g, 2.85 mol) and AA (4.2890 mL aqueous solution containing 10.9 mg or 0.147 mmol AA) under stirring at 200 rpm in a 250-mL flask. Parallel to this, an AIBN (27.1 mg, 0.165 mmol) solution in styrene (3.46 g, 33.2 mmol) was prepared and added to the suspension. The whole mixture was kept under permanent stirring at room temperature for a total of 20 min. Only after this, a water bath preheated to 80 °C was placed underneath the reaction vessel to start the polymerization. The reaction mixture was kept at this temperature for a total of 7 h.

Methods

Purification of the polymer dispersions

All polymer dispersions were purified by exhaustive dialysis against water through a Spectra/Por 7 dialysis membrane (MWCO 50 kDa, Spectrum Laboratory Products Inc., New Brunswick, New Jersey, USA) before characterization, but not between individual synthesis steps.

Electron microscopy

Field-emission scanning electron microscopy (FESEM) images were obtained using a Gemini 500 microscope (Carl Zeiss AG, Oberkochen, Germany) operating at 3 kV. Parallel to this, transmission electron microscopy (TEM) images were used to confirm that the FESEM images can be used to determine the lobe sizes of the particles analyzed here. The TEM images were taken using a Libra 120 TEM microscope (Carl Zeiss AG) operating at 120 kV. A comparison between the results obtained from both methods and justification for the use of FESEM in the morphological analysis are presented in Section S1. The particle analysis was done using macros from the software ImageJ (National Institutes of Health, US Department of Health and Human Services, Washington, D.C., U.S.A), and the data obtained with ImageJ was analyzed from there on using custom software. At least 500 particles were measured for each numerical data item shown below.

Density measurements

The density of the spherical particles was determined at 20 °C using a DMA 5000 M density meter (Anton Paar Group AG, Graz, Austria). A total of 10 density measurements were performed for suspensions of varying particle concentrations ranging from 0.5 to 5%(m/m). The particle densities were calculated by extrapolating of the reciprocal values of the suspension densities (specific volumes) to a particle content of 100%(m/m).

Differential centrifugal sedimentation

Differential centrifugal sedimentation (DCS) was employed to determine the sedimentation coefficients of the particles. Measurements were performed in an ultra-high-resolution disk centrifuge (DC 24000 UHR, CPS Instruments, Prairieville, Louisiana, USA) equipped with an on-board balancing system. Separation of the particles according to their sedimentation coefficients was performed at 24,000 rpm and 30 °C. Particle detection was performed at 405 nm using an integrated low-noise laser light source and detector system. The disk was loaded with a sucrose density gradient ranging from 8%(m/m) on the outermost layer to 2%(m/m) on the innermost gradient layer, totaling a volume of 14.4 mL. The aqueous gradient was covered with 0.5 mL dodecane to avoid evaporation of the aqueous gradient. All samples were treated by ultrasonication immediately before being loaded onto the density gradient. The sedimentation coefficients for the samples were determined by the time between the start of the experiment and the detection of the particles at a fixed position. Profiles of the sedimentation coefficients can be seen in Fig. S2 in Section S2. [21]

Results and discussion

Surface modification can be used in seeded polymerizations to limit the swelling of polymer particles with monomer. The latter has proven as an appropriate means of triggering the formation of a monomer protrusion and therefore ultimately anisotropic growth [8, 15]. The same can be achieved by cross-linking of the seed particles resulting in a segregation of monomer from the cross-linked seed. In the latter case, this strategy was expanded in pursuit of particles with higher degrees of anisotropy and complexity. This was accomplished by conducting a second lobe-forming seeded polymerization. The driving force controlling the final particle morphology was a gradient in the cross-linking densities between the two lobes of the dumbbell particles used as seeds [20]. It therefore seems likely that a gradient in surface wettability generated by a hydrophilic surface modification could also steer protrusion formation in a preferred direction. In the following, it will be thus studied if gradients in surface coatings are an effective means for the fabrication of particles composed of three individual lobes aligned in one direction.

General procedure

The hypothesis that a gradient in surface wettability can produce a new lobe aligned with the ones of dumbbell-shaped seed particles will be examined based on colloidal particles prepared by the synthesis pathway shown in Fig. 1A. At first, spherical polystyrene latex particles (sample S) were prepared by emulsion polymerization of styrene. The narrow size distribution of the particles is reflected by FESEM micrographs (Fig. 1B). In the second step, the particles were coated with a surface layer made from the silane-based comonomer MPS. The surface modification was accomplished by seeded copolymerization of styrene and MPS. The narrow size distribution already observed for sample *S* continues to be reflected in the modified spherical particles, designated as sample MS (Fig. 1C). This shows the absence of secondary nucleation and underlines the homogeneous growth of the polymer particles.

Although the procedure for making the surface modification is well-established [11, 22, 23], there are a few essential aspects to be noted aiming towards a better understanding of subsequent synthesis steps. The silane groups are preferentially located at the surface of the MS particles. This is due to the higher hydrophilicity of MPS as compared to styrene. The silane coating renders the surface of the polystyrene latex particles more hydrophilic, thus limiting the wettability and swellability of the particles when monomer is added [15]. In line with earlier reports, it should be noted that just making the surface of a given particle hydrophilic is not enough to promote the phase separation and protrusion formation [14]. The requirement to make the phase separation and protrusion formation take place has proven to be directly related to the use of specific comonomers. For this purpose, MPS is used as a comonomer and functionalizing agent in this study. The introduction of MPS by copolymerization with styrene in a seeded polymerization helps to achieve a defined silane layer at the particle surface [15]. This procedure has already been described for copolymerization processes using different trimethoxysilyl-containing monomers [11, 15]. Variations in the amount of the comonomer have been made enabling adaptions to different sizes [11, 15]. Like what has been observed for cross-linked particles [19], the concentration of the comonomer must be adjusted for the size of the particles so that the formation of a protrusion can be guaranteed. The amount of MPS used here for the functionalization of sample S and formation of MS (3.45 mol% with regard to total styrene used during the first and second synthesis steps) was chosen in an adequate range for their dimensions [24].

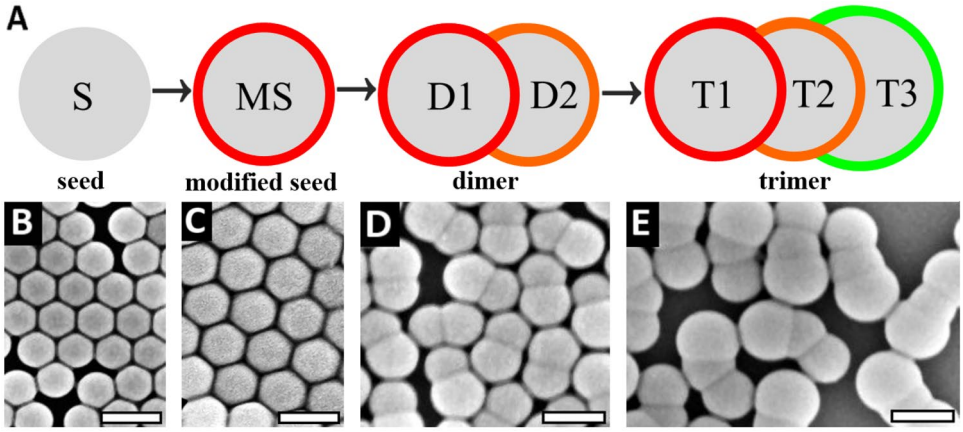

Fig. 1 **A** Strategy for the fabrication of three-lobed polymer particles based on consecutive seeded polymerizations. At first, narrowly dispersed polystyrene latex particles were prepared by emulsion polymerization (sample S). The spherical particles were coated with a silane layer (sample MS; surface layer highlighted in red) in a first seeded polymerization. The surface coating limited the wettability with the monomer in a subsequent seeded polymerization, creating a monomer protrusion that was converted into a new lobe attached to the MS seed particle during the polymerization reaction. The surface of the D2 lobe of the dumbbell-shaped particles (sample D) was also covered with a silane coating (orange), albeit to a lesser extent of silane groups. The gradual difference in the surface functionalization between lobes D1 and D2 controls the direction of nucleation and growth of further monomer protrusions in a third-seeded polymerization, yielding particles with three individual lobes (sample T). During the polymerization, selective functionalization of the trimer lobe T3 (green) is possible. **B**-**E**: FESEM micrographs of particles collected in each of the four synthesis steps are shown below the corresponding schematic representation. The scale bars represent 200 nm. Particles from all samples have defined shapes and narrow size distributions (see also Fig. S3). A high level of uniformity already anchored in the initial seed particle S is thus fully preserved over the course of three subsequent seeded polymerizations. Most remarkably, the trimer particles T exhibit a high degree of linearity, indicating the directional control on the formation of the monomer protrusion by the wettability gradient during synthesis

To return to Fig. 1A, the spherical MS particles are used as seeds to make dumbbell-shaped polymer particles (sample D). The latter are prepared in a second seeded emulsion polymerization. It is important to differentiate between the first seeded polymerization (for making MS particles) and the second one yielding dumbbell particles D. In the first case, there is spherical growth mediated by seeds swollen with monomer without formation of a protrusion. By contrast, monomer protrusions are expected to develop due to the limited wettability of the MS particles with monomer. The lower wettability results also in a decreased swellability. The latter is observed when heating the particles [16]. For the sake of simplicity, the protrusion-forming seeded emulsion polymerization is hereinafter referred to as anisotropic seeded polymerization (ASP) due to its key feature to drive growth into an anisotropic direction.

With the goal of making three-lobed particles in mind, the new lobes of the dumbbell particles D were also equipped with a thin silane coating. The latter was, once more, achieved by copolymerization of styrene and MPS, but now in the context of ASP. This means that the actual copolymerization proceeds within the monomer protrusion, thus providing the possibility for targeted functionalization of the freshly formed lobe. The complete transformation of spherical particles into anisotropic dumbbell-shaped particles was observed, as indicated by the absence of spherical particles in FESEM micrographs of sample D. Furthermore, the dumbbells exhibited a low dispersity and were uniform in their shape as well (Fig. 1D). This again demonstrates that the dispersity of the seed particles is preserved during the ASP step.

As already mentioned, the purpose of using MPS one more time during the formation of the dimers D was to synthesize particles capable of promoting a new protrusion formation, like during the preparation of MS particles. In this step, the MPS concentration was kept at 2.13 mol% with regard to the styrene added during dumbbell synthesis. It is known from earlier reports on making dumbbell particles that this quantity is still sufficient to promote the formation of monomer protrusions [11].

Having two different MPS concentrations on each of the two dumbbell lobes creates a wettability gradient between them, whilst still keeping the overall MPS amount high enough to promote the formation of protrusions. This paved the way for making three-lobed particles (T) in a second ASP reaction. The third lobe was made by copolymerization of styrene and a small amount of acrylic acid to improve the colloidal stability of the dispersion. Virtually full conversion from two-lobed species into three-lobed particles

Table 1 Average sizes and related standard deviations for the spherical S and MS particles

	FESEM		TEM		DCS	
	d_n(nm)	*PDI*	d_n (nm)	*PDI*	d_n (nm)	*PDI*
S	132	1.0016	134	1.0011	132	1.0096
MS	163	1.0016	166	1.0016	156	1.0029

d_n denotes the number-averaged diameter as measured by using complementary techniques; PDI represents the polydispersity index, which is defined as the weight-averaged particle diameter divided by the number-averaged particle diameter

was observed (Fig. 1E), indicating an effective formation of monomer protrusions during ASP. In terms of figures, 99% of the particles in sample T had three individual lobes.

Both in the case of samples D and T, the formation of a solid rounded lobe during their syntheses clearly demonstrates that the degree of surface functionalization on their seeds was sufficient to promote the formation of monomer protrusions. Furthermore, the high level of linearity of the three-lobed particles T suggests that the wettability gradient must have steered the protrusion formation, in line with previous findings for cross-linked particles [12]. In accordance with what was observed for the dumbbells D, uniform shapes and a low dispersity were also observed for the trimers T (Fig. 1E). This once more shows that high levels of shape uniformity can be preserved over multiple seeded polymerizations reactions [15], thus opening up perspectives for a step-by-step fabrication of colloidal nanoparticles with custom-tailored geometries.

Seed and lobe diameters

For more detailed insights, the particle dimensions were analyzed for samples S, MS, D, and T. For the determinations of the lobe sizes of samples D and T, the particles were considered to consist of overlapping spheres, following the lines of previous reports [16, 25]. The data regarding the size and dispersity of the spherical S and MS particles is summarized in Table 1. Corresponding data for the lobes of the two- and three-lobed particles D and T is gathered in Table 2.

Analysis of FESEM images of the samples S and MS revealed number-averaged diameters (d_n) of 132 nm and 163 nm. The larger diameter of the MS particles when compared to S indicates the growth of the particles during the seeded polymerization used to establish the silane coating. *PDI* values were 1.0016 for both sets of spherical particles. These low *PDI* values corroborate a narrow size dispersity, as also seen in the corresponding histograms (Fig. S3A for sample S; Fig. S3B for sample MS). The narrow size dispersity is expected for products of emulsion polymerization. Having a narrow seed distribution is essential to be carried forward to the products of subsequent seeded polymerizations [15]. A high regularity in size and shape was also observed by TEM (Fig. S1) and DCS (Fig. S2). In the first case, d_n was found to be 134 nm and 166 nm for S and MS, respectively, with *PDI* values of 1.0011 and 1.0016. d_n as determined using DCS for S and MS was 132 nm and 156 nm, correspondingly, whereas the *PDI* for these samples were determined to be 1.0096 and 1.0029. The density values (ρ) measured for S and MS (1.054 g mL^{-1} and 1.073 g mL^{-1}) were used to calculate d_n for these samples from their sedimentation coefficients determined by DCS. As expected, the particle density observed for sample S was close to the one reported for solid polystyrene [26]. Due to the silane coating, the density of the MS particles was significantly higher, reflecting the effective incorporation of silane groups during the surface functionalization. The affirmation that the narrow size dispersity is carried from the seeds to the particles prepared from them is also backed

Table 2 Average sizes and related standard deviation values for the D and T samples

D	$d_{D,av.}$ (nm)	*PDI*	$d_{D,small}$ (nm)	*PDI*	$d_{D,large}$ (nm)	*PDI*	$l_{D1,D2}$ (nm)	*SD* (nm)				
	168	1.0064	158	1.0036	178	1.0023	100	11				
T	d_{T1} (nm)	*PDI*	d_{T2} (nm)	*PDI*	d_{T3} (nm)	*PDI*	$l_{T1,T2}$ (nm)	*SD* (nm)	$l_{T2,T3}$ (nm)	*SD* (nm)	$l_{T1,T3}$ (nm)	*SD* (nm)
	170	1.0033	168	1.0044	204	1.0018	109	12	100	13	201	18

d_i is the number-averaged diameter as measured for the lobe i; $l_{li,j}$ denotes the number-averaged center-to-center distance between the lobes i and j; PDI represents the polydispersity index of the lobe diameters; it is defined as the weight-averaged diameter divided by the number averaged diameter; *SD* denotes the standard deviation for the distances measured. Please note that a clear specification of the D1 and D2 lobes according to their actual role in the consecutive polymerizations was not possible due to the similarity of their sizes. As the dumbbell lobes D1 and D2 are nearly equal in size, the diameter $d_{v,av.}$ averaged over both lobes is shown instead of mean diameters for individual lobes. In addition, a classification of the dumbbell lobes by size was made, yielding the number-averaged sizes of the smaller and the larger dumbbell lobes ($d_{D,small}$ and $d_{D,\ large}$). It should be noted that a clear allocation to the lobes D1 and D2 by size is not possible. See text for further explanation

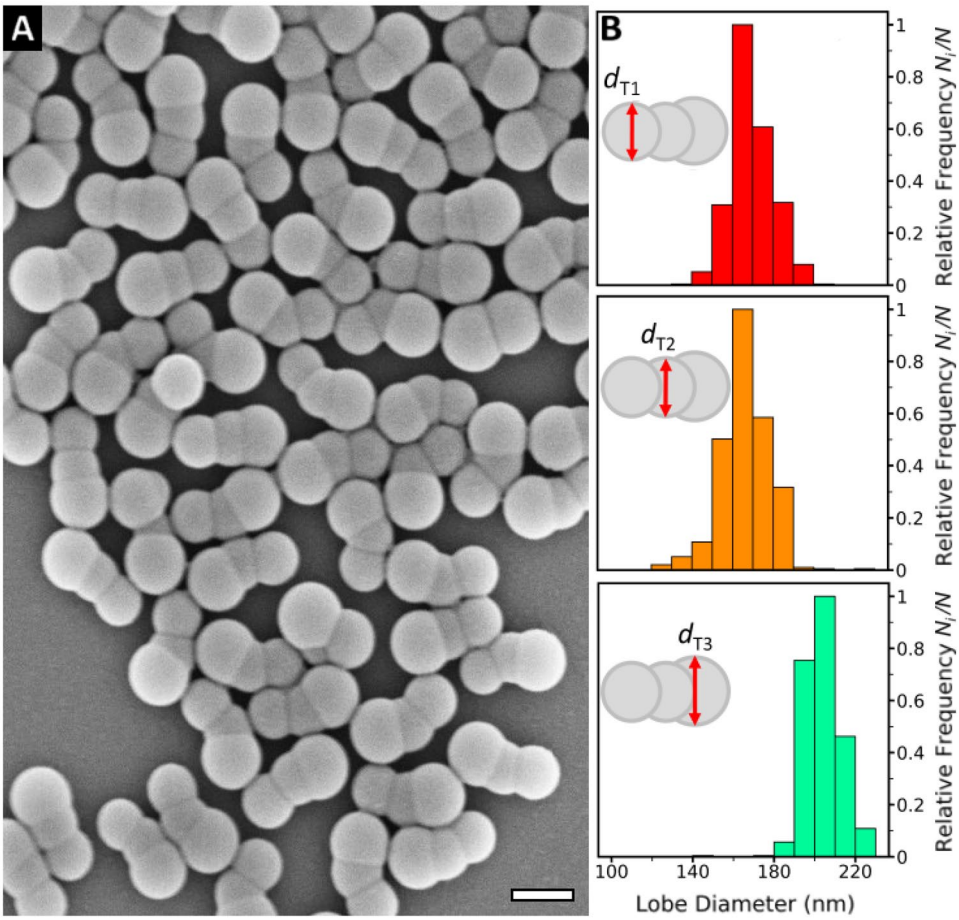

Fig. 2 Spatial dimensions of the trimer particles T. **A** FESEM image of the trimer particles, sample T. The particles have defined shapes, and the three lobes can be clearly distinguished. The scale bar represents 200 nm. **B** Distributions of the diameters of the individual lobes of the trimers determined from a total of 500 particles. These are the lobe diameter distributions for the smaller extremity lobes T1 (top), for the middle lobes T2 (center), and for the larger trimer extremity T3 (bottom). The relative frequencies (N_i/N) displayed in the histogram are normalized to the most frequently occurring lobe diameters. In all three cases, narrow distributions are observed, indicating the low dispersity of the seed particles being transmitted over the seeded polymerizations to the trimers

by the analysis of the dimer particles D. It has to be clearly noted that when analyzing the microscopy images of the dumbbells, it was not possible to distinguish between the lobes D1 and D2. Variations in mean sizes are small. This is reflected by a monomodal size distribution when analyzing both sets of lobes together (Fig. S3C). Even though a clear allocation of the lobes was not feasible, the monomodal distribution could be split into two subdistributions representing the size distributions of the smaller and larger halves of the dumbbells (Figs. S3D and S3E). The resulting mean values $d_{D,small}$ and $d_{D,large}$ differed by just 10 nm from the mean diameter averaged over all lobes ($d_{D,Avg} = 168$ nm, $PDI = 1.0064$). The dumbbell lobes showed low dispersities in size, even when averaged over both types of lobes. Moreover, the distribution of the sedimentation coefficients of the dimers (Fig. S2) also underlines the low dispersity of the dumbbells in terms of size and shape. Interestingly, the diameters found for the dumbbell lobes indicate little to no growth during the ASP from MS. Moreover, the dumbbell lobes had roughly the same size as the MS particles used as seeds. Furthermore, it should be noted that the amount of monomer consumed during the dumbbell synthesis was similar to the mass of the MS particles used as seeds. This demonstrates that the monomer was expelled from the seed during ASP. Instead, the monomer had been fully transferred to the monomer protrusion that was solidified during the polymerization yielding dumbbells with lobes of similar sizes. As mentioned above, the latter finding hampers a clear distinction among the lobes D1 and D2, justifying the size analysis being made in Table 2 omitting any assignment to lobes D1 and D2. In other words, a classification of the lobes according to their wettability can only be made at the level of the trimers.

Turning to the trimer particles, the dimensions of the two smaller lobes, T1 ($d_{T1} = 170$ nm, $PDI = 1.0033$) and T2 ($d_{T2} = 168$ nm, $PDI = 1.0044$) were like those observed for the dumbbell lobes, as reflected in the quantity $d_{D,av}$. Analogous to the findings with the dimers, this demonstrates that there was little to no growth when compared to their initial sizes before the ASP (Table 2). This means that the added monomer was mostly expelled from the dumbbell-shaped seeds, thus forming the third and largest lobe T3 ($d_{T3} = 204$ nm, $PDI = 1.0018$). The same was found with respect to their narrow lobe size distributions (Fig. 2B),

indicating the preservation of dimensional uniformity from the previous steps. The new lobes T3 had narrowly dispersed diameters as well (Fig. 2B). Rather like for the two-lobed particles, the uniformity for the three-lobed particles was further corroborated by their narrow sedimentation coefficient distribution (Fig. S2). The larger size observed for the T3 lobe in comparison to the other lobes reflects the high styrene quantity used to promote the protrusion formation. This was done to enable an easy identification of the T3 lobes formed in the last step of three consecutive seeded polymerizations.

Lobe distances

Colloidal particles with complex and yet defined shapes such as the three-lobed particles are of interest as building units for hierarchical superstructures [3] and to explore the hydrodynamic behavior of complex nanoparticles [2, 27]. In view of a further analysis of the particle shape, FESEM images were used to determine the distances between the centers of the lobes for the dimers D and the trimers T as well as the standard deviations for the related distributions. The distribution of the distances between the lobes D1 and D2 (mean value $l_{D1,D2} = 100$ nm, $SD = 11$ nm) is shown in Fig. 3A.

For the trimer particles T, the lobe distance distributions between T1 and T2 ($l_{T1,T2,\,n} = 109$ nm, $SD = 12$ nm), T2 and T3 ($l_{T2,T3,\,n} = 100$ nm, $SD = 13$ nm), and T1 and T3 ($l_{T1,T3,\,n} = 201$ nm, $SD = 18$ nm) are shown in Fig. 3B, C, and D. In addition, mean values of the lobe distances are summarized in Table 2. A bimodal distribution was observed for the distances $l_{T1,T3}$ among the first and third lobe of the trimers (Fig. 3D). The minor mode below 160 nm is representing a small percentage of closed trimers, whereas most of the trimers exhibited elongated configurations, as reflected by larger $l_{T1,T3}$ values.

The mean distance between the centers of the first two lobes of the trimers T ($l_{T1,T2}$) was comparable to the distance between the corresponding lobes of the seed particles D ($l_{D1,D2}$). Moreover, the lobes T1, T2, D1, and D2 have comparable sizes, which is a further indication that the first two were formed from the latter ones. This means that the dumbbell lobes D1 and D2 were transformed into the trimer lobes T1 and T2 with minor changes to their morphology and size. Regardless of the larger size of lobe T3 when compared to lobes T1 and T2, $l_{T1,T2}$ was still observed to be larger than $l_{T2,T3}$. This observation is related to the higher hydrophilicity of lobe T1 (the former seed during dumbbell synthesis) when compared to T2. A higher hydrophilicity leads to a lower affinity between the seed particle and the monomer protrusion formed on its surface [14]. Ultimately, this results in a higher degree of separation between the former dumbbell lobes T1 and T2 as compared to T2 and the new lobe T3. This is also reflected in a larger contact area between T2 and T3 than between T1 and T2. The lobe distance distributions for the dimers and trimers thus corroborate once more the assumption that the last lobe to be formed is the largest one, referred to as T3. In other words, it can be clearly excluded that the largest trimer lobe T3 could have been formed by the growth of either D1 or D2.

Trimer angle distributions

As stated above, most trimers were found to have extended configurations. To quantify the linearity of the obtained

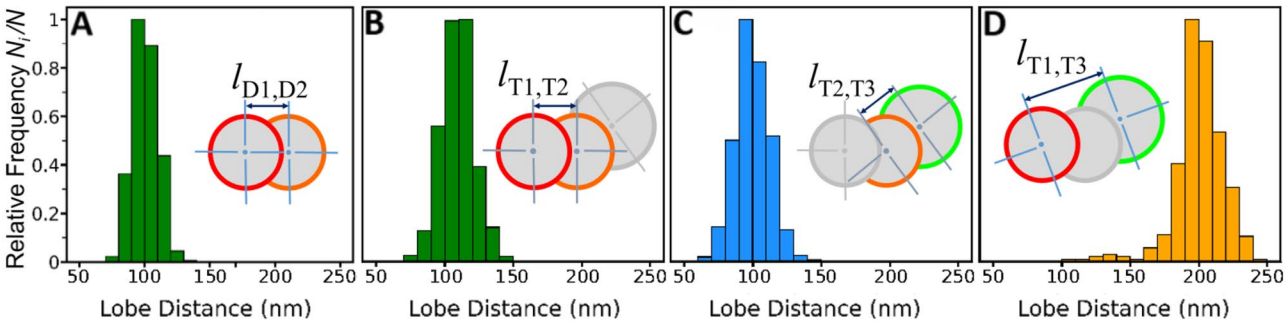

Fig. 3 Distances between the lobes of the dimers and trimers. **A** Lobe distance $l_{D1,D2}$ distributions as measured for the dumbbells; **B** to **D** distance distributions between the various trimer lobes. See insets for an illustration of the measured distances $l_{T1,T2}$, $l_{T2,T3}$, and $l_{T1,T3}$. The histograms highlight that the distances between the centers of the dumbbell lobes are comparable to those between the two smaller lobes of the trimers, T1 and T2. Together with their size distributions, this finding demonstrates that D1 and D2 were transformed into T1 and T2 during the synthesis of the trimers by ASP. All distributions are narrow, reflecting the morphological uniformity of the samples presented. A bimodal distribution was observed for the distances $l_{T1,T3}$. The vast majority of trimers can be identified as the population for which $l_{T1,T3} > 160$ nm. This population can be defined as elongated or open trimers because there is no mutual contact between T1, T2, and T3. The minor population with $l_{T1,T3} < 160$ nm comprises compact or closed trimers, characterized by mutual contact between T1, T2, and T3

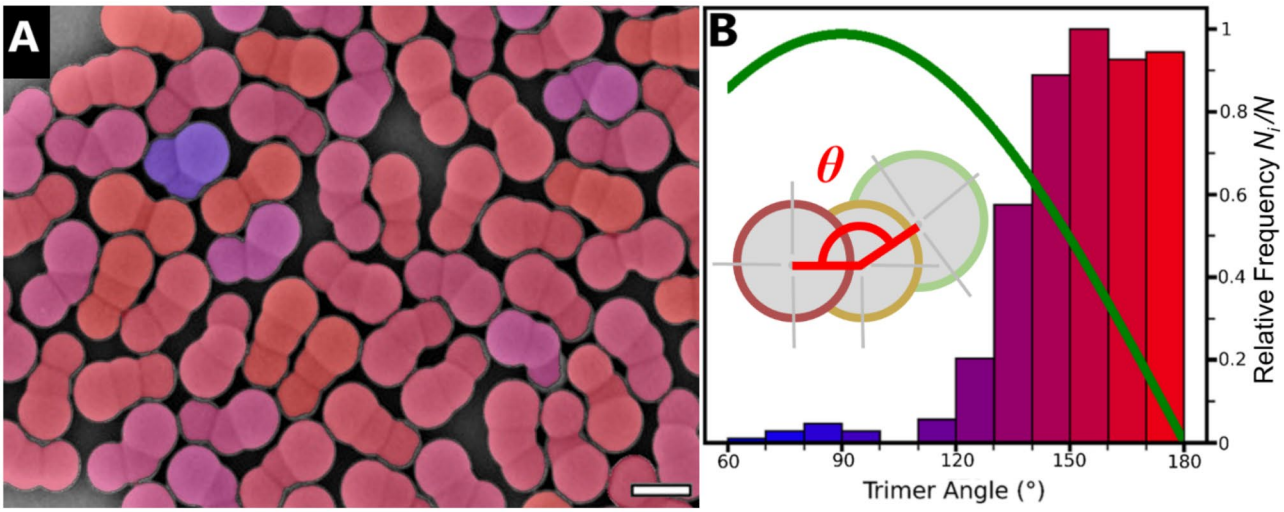

Fig. 4 Angle distribution of the three-lobed particles. **A** Color-coded FESEM image with a scale bar representing 200 nm. The trimers are color-coded according to their angles θ. The same color scheme is used in the experimental angle distribution. **B** Comparison of the experimental angle distribution (color-coded histogram) with the hypothetical distribution (green line) expected for random lobe nucleation during ASP (see S4). The angle θ denotes the largest angle between the centers of lobes T1, T2, and T3. In this scenario, 180° represents ideal linearity. The majority of the trimers were found to be almost linear. This demonstrates once more that the formation of their shape was controlled by the wettability gradient between the D1 and D2 lobes of the two-lobed seeds

trimer particles, FESEM images were further employed to measure the angle between the centers of the three lobes (θ). One of these FESEM images is shown in Fig. 4A, in which the three-lobed particles can be identified by an angle-dependent color code. This code follows the colors used in the angle distribution histogram (Fig. 4B). The high degree of linearity observed for the trimer particles T ($\theta_n = 154$, $SD = 19°$) signals that the gradient in functionalization density between D1 and D2 was sufficient to steer the protrusion formation to a linear direction during the ASP reaction, resulting in an alignment of the lobes T1, T2, and T3. This observation follows the formation of three-lobed particles driven by a gradient in cross-linking density [20]. Assuming a random nucleation of protrusions on the D2 lobe, one would expect an angle distribution described by a sine function (see section S4 of the SI, Figs. S4, S5, and S6 for further explanation). The comparison between a hypothetical random angle distribution and the experimentally observed distribution (Fig. 4B) clearly shows that the gradient in surface wettability promoted linear growth.

The minor population of closed trimers already identified during the evaluation of lobe distances (Fig. 3) can also be found in the angle distribution (Fig. 4B). The small population of closed trimers is reflected in angles below 100°. However, it should be noted once more that 99% of the trimer particles exhibited elongated, almost linear configurations. It is to be expected that even higher degrees of linearity could be achieved by using steeper wettability gradients, given that wettability as a driving force to promote protrusion formation continues to show similarities with earlier efforts based on cross-linking [12].

Complementary to the angle distribution, Fig. S7 shows the distributions of the aspect ratios (*AR*) for the dimers D and trimers T. The *AR* values denote the length-to-width ratios of the anisotropic polymer colloids. As expected, the aspect ratios were significantly higher for the three-lobed particles in comparison to the two-lobed ones. It should be emphasized that the high proportion of T particles with aspect ratios above 2.0 is in line with linear growth during the second ASP process. *AR* values between 1.5 and 1.7 can be attributed to the small fraction of closed trimers observed in the trimer sample. The high level of anisotropy of the vast majority of the three-lobed particles is expected to exert a significant impact on their phase behavior and structure formation. It will be beneficial with regard to their alignment into organized superstructures such as colloidal crystals with reduced symmetries at the lattice points [8].

Mechanistic explanation for regio-selective particle growth

A first evaluation of the mechanism that promotes the linear growth of seed particles with gradients in surface wettability can be made at this point. The following explanations are in full accord with the experimental findings shown above. The mechanistic considerations are inferred from analogy based

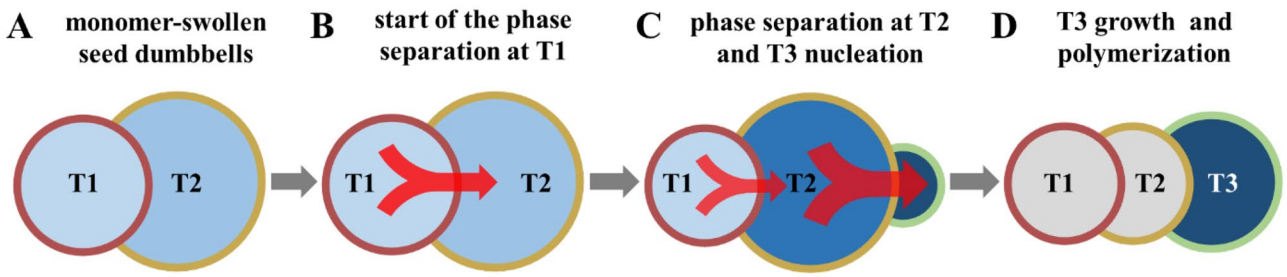

Fig. 5 Scheme of the mechanism of new protrusion nucleation and linear trimer formation. **A** At the beginning, the seed dumbbells are in a saturation swelling equilibrium where the contributions to the free energy are well balanced. **B** Heating during polymerizations increases the elastic retractile force of the swollen polymer chains, thus promoting the formation of a monomer protrusion. Relaxation of the polymer chains starts at lobe T1 because of the higher volume fraction of the polymer. Consequently, the monomer is expelled from lobe T1 and transported to lobe T2. **C** At this point, further swelling of the lobe T2 is unfavorable because of the increasing retractile force. A phase separation will take place inside lobe T2 before the one taking place in lobe T1 is completed. The monomer that was originally inside lobe T1 is transported into lobe T2, making the monomer expelled from lobe T2 move in the same direction. This leads to the formation of lobe T3 in a linear configuration with the other lobes. The growth of the nucleated lobe T3 is expected to happen in an almost instantaneous manner, leading to a monomer droplet attached to the surface of lobe T2. **D** Finally, the polymerization and solidification of the new monomer protrusion will proceed while preserving the linear morphology created in the previous steps. The lobes are color-coded according to the volume fraction of the monomer inside. Darker blue indicates a higher volume fraction of monomer. Red arrows represent the monomer flux

on the conceptual similarity to known cases where linear particle growth had been mediated through gradients in the crosslinking density of the seed particles [20].

As mentioned in the introduction, the formation of a liquid protrusion upon swelling of the polymer seed with monomer can be explained by the interplay of three contributions to the free energy. While the free energy of mixing the monomer with polymer promotes swelling, the surface tension of the seed particle with the aqueous phase and the stretching of the polymer chains restrict the swelling of the seed particle [14]. The heating during seeded polymerization increases the elastic retractile force of the swollen polymer chains. This increase in the elastic energy of the polymer chains results in an overall positive value of the total free energy, which is given as the sum of the contributions mentioned above. The positive free energy promotes a phase separation between monomer and polymer, leading to the formation of a monomer protrusion attached to the seed particle [28].

With regard to the formation of the trimers, the volume fractions of polymer across the two-lobed seed are inversely related to the swelling degrees of the two lobes. It is to be expected that the lobe with the lower surface wettability is swollen to a lower extent. Similar considerations were made for cross-linked particles where the degree of swelling can be formulated by the Flory-Rehner theory [17, 18]. Expanding on this consideration, a lower local surface wettability also decreases the sol fraction, a value that defines the fraction of unreacted monomer and soluble chain segments formed during polymerization. The opposite of the sol fraction is the gel fraction, in this context understood as the volume fraction of entangled macromolecules within the two lobes [29]. A lower local surface wettability, thus resulting in a higher gel fraction, is associated with shorter relaxation times of the swollen polymer lobe. Lower surface wettability thus accelerates the phase separation process during polymerization [17, 28].

Considering monomer-swollen dumbbells as seeds with two halves varying in surface wettability, the lobe with the lower surface wettability will have a shorter relaxation time (Fig. 5A). Consequently, this lobe will undergo phase separation under heating first, accompanied by the transportation of the monomer into the other lobe with the higher surface wettability. This flux towards the lobe with the higher surface wettability (T2) favors the phase separation proceeding on the surface of lobe T2 (Fig. 5B). In line with the experimental observations, the new lobe T3 is thus expected to grow adjacent to the dumbbell lobe with the highest surface wettability under alignment to the direction of monomer flux within the dumbbell seed (Fig. 5C). It is for this reason that the direction of monomer transportation points to the site at which the monomer protrusion is formed. It is known that the formation of the monomer protrusion takes place in an almost instantaneous manner, meaning that it is possible to observe either fully-grown protrusions or none by cryogenic electron microscopy [16]. Hence, the phase separation is a fast-proceeding process, and the formation of a monomer protrusion activates a monomer flow in the direction of the site where the protrusion is being formed. This finally produces the linear growth observed in the experiments (Fig. 5D).

Conclusions

Specific surface coatings can become a limiting factor that restricts the swelling of polymer particles. Taking advantage of this effect opens up avenues to direct seeded polymerization into an anisotropic dimension. Regio-specific formation of new polymer lobes can be accomplished when using seed particles, which exhibit gradients in surface wettability. Two-lobed particles with dumbbell-shaped morphologies can serve as anisotropic seed particles. Because the two lobes are prepared one by one, varying degrees in surface functionalization can be achieved, thus yielding the required gradient in surface wettability. This provides the basis to further reinforce the anisotropic nature of the colloidal seed particles by adding a new lobe along their main symmetry axis.

While the above study has shown the practical implementation of the strategy, further progress regarding improvements in linearity is still to be expected from the optimization of the surface gradient. It is worth noting that other aspects such as the size of the seed particles or external parameters such as temperature could also affect the overall quality of protrusion formation. Other new directions include the extension of the strategy to make multi-segmented hybrid particles synthesized from different monomers. Moreover, specific surface functionalization of the most recently formed lobe should open avenues with respect to asymmetric functionalization of the shape-anisotropic colloids.

Supplementary Information The online version contains supplementary material available at https://doi.org/10.1007/s00396-023-05131-z.

Acknowledgements Technical support from the Nanostructure Laboratory (nano.lab) and the Particle Analysis Centre (PAC) at the University of Konstanz is gratefully acknowledged.

Author contribution Conceptualization: GAAM, AW; methodology: GAAM, AW; formal analysis and investigation: GAAM, AW; writing—original draft preparation: GAAM, AW; writing—review and editing: GAAM, AW; funding acquisition: AW; resources: AW; supervision: AW.

Funding Open Access funding enabled and organized by Projekt DEAL. This research was funded by the DEUTSCHE FORSCHUNGSGEMEINSCHAFT within SFB 1214/B4.

Data availability The datasets generated during the study are available from the corresponding author upon reasonable request.

Declarations

Conflict of interest The authors declare no competing interests.

References

1. Maldiney T, Richard C, Seguin J et al (2011) Effect of core diameter, surface coating, and PEG chain length on the biodistribution of persistent luminescence nanoparticles in mice. ACS Nano 5:854–862. https://doi.org/10.1021/nn101937h
2. Stuckert R, Plüisch CS, Wittemann A (2018) Experimental assessment and model validation on how shape determines sedimentation and diffusion of colloidal particles. Langmuir 34:13339–13351. https://doi.org/10.1021/acs.langmuir.8b02999
3. Zhang Q, Zeng S, Lin B, Qin J (2011) Controllable synthesis of anisotropic elongated particles using microvalve actuated microfluidic approach. J Mater Chem 21:2466–2469. https://doi.org/10.1039/c0jm04033a
4. Erni P, Cramer C, Marti I et al (2009) Continuous flow structuring of anisotropic biopolymer particles. Adv Colloid Interface Sci 150:16–26. https://doi.org/10.1016/j.cis.2009.05.005
5. Ten Brinke AJW, Bailey L, Lekkerkerker HNW, Maitland GC (2008) Rheology modification in mixed shape colloidal dispersions. Part II: Mixtures Soft Matter 4:337. https://doi.org/10.1039/b713144e
6. Glotzer SC, Solomon MJ (2007) Anisotropy of building blocks and their assembly into complex structures. Nat Mater 6:557–562. https://doi.org/10.1038/nmat1949
7. Plüisch CS, Wittemann A (2013) Shape-tailored polymer colloids on the road to become structural motifs for hierarchically organized materials. Macromol Rapid Commun 34:1798–1814. https://doi.org/10.1002/marc.201300693
8. Forster JD, Park JG, Mittal M et al (2011) Assembly of optical-scale dumbbells into dense photonic crystals. ACS Nano 5:6695–6700. https://doi.org/10.1021/nn202227f
9. Sturm E, Cölfen H (2017) Mesocrystals: past, presence, future. Crystals (Basel) 7:207. https://doi.org/10.3390/cryst7070207
10. Wagner CS, Fischer B, May M, Wittemann A (2010) Templated assembly of polymer particles into mesoscopic clusters with well-defined configurations. Colloid Polym Sci 288:487–498. https://doi.org/10.1007/s00396-009-2169-y
11. Stuckert R, Lüders A, Wittemann A, Nielaba P (2021) Phase behaviour in 2D assemblies of dumbbell-shaped colloids generated under geometrical confinement. Soft Matter 17:6519–6535. https://doi.org/10.1039/D1SM00635E
12. Désert A, Chaduc I, Fouilloux S et al (2012) High-yield preparation of polystyrene/silica clusters of controlled morphology. Polym Chem 3:1130–1132. https://doi.org/10.1039/c2py20058a
13. Désert A, Morele J, Taveau JC et al (2016) Multipod-like silica/polystyrene clusters Nanoscale 8:5454–5469. https://doi.org/10.1039/c5nr07613g
14. van Ravensteijn BGP, Kegel WK (2017) Tuning particle geometry of chemically anisotropic dumbbell-shaped colloids. J Colloid Interface Sci 490:462–477. https://doi.org/10.1016/j.jcis.2016.11.045
15. Park JG, Forster JD, Dufresne ER (2010) High-yield synthesis of monodisperse dumbbell-shaped polymer nanoparticles. J Am Chem Soc 132:5960–5961. https://doi.org/10.1021/ja101760q
16. Stuckert R, Krumova M, Wittemann A (2022) Cryogenic transmission electron microscopy for observation of monomer protrusions that emerge during formation of dumbbell-shaped polymer

colloids. Colloid Polym Sci 300:1257–1267. https://doi.org/10.1007/s00396-022-05000-1
17. Sheu HR, El-Aasser MS, Vanderhoff JW (1990) Phase separation in polystyrene latex interpenetrating polymer networks. J Polym Sci A Polym Chem 28:629–651. https://doi.org/10.1002/pola.1990.080280314
18. Kim JW, Larsen RJ, Weitz DA (2006) Synthesis of nonspherical colloidal particles with anisotropic properties. J Am Chem Soc 128:14374–14377. https://doi.org/10.1021/ja065032m
19. Mock EB, de Bruyn H, Hawkett BS et al (2006) Synthesis of anisotropic nanoparticles by seeded emulsion polymerization. Langmuir 22:4037–4043. https://doi.org/10.1021/LA060003A
20. Kim J-W, Larsen RJ, Weitz DA (2007) Uniform nonspherical colloidal particles with tunable shapes. Adv Mater 19:2005–2009. https://doi.org/10.1002/adma.200602345
21. Scott DJ, Harding SE, Rowe AJ (2005) Introduction to differential sedimentation. In: Scott DJ, Harding SE, Rowe AJ (eds) Analytical Ultracentrifugation. Royal Soc Chem 270–290
22. Ni K, Shan G, Weng Z (2007) Partition of 3-trimethoxysilyl propyl methacrylate in emulsion polymerization system. Acta Polymerica Sinica 38–41. https://doi.org/10.3724/SP.J.1105.2007.00038
23. Sun Y, Zhang H, Han W et al (2019) Controllable synthesis of monodisperse nonspherical colloidal particles with cavity structures. J Polym Sci, Part A: Polym Chem 57:1645–1652. https://doi.org/10.1002/pola.29429
24. Chu F, Siebenbürger M, Polzer F et al (2012) Synthesis and characterization of monodisperse thermosensitive dumbbell-shaped microgels. Macromol Rapid Commun 33:1042–1048. https://doi.org/10.1002/MARC.201200062
25. Peng B, van Blaaderen A, Imhof A (2013) Direct observation of the formation of liquid protrusions on polymer colloids and their coalescence. ACS Appl Mater Interfaces 5:4277–4284. https://doi.org/10.1021/am400490h
26. Plüisch CS, Stuckert R, Wittemann A (2021) Direct measurement of sedimentation coefficient distributions in multimodal nanoparticle mixtures. Nanomaterials 11:1027–1045. https://doi.org/10.3390/nano11041027
27. Hoffmann M, Wagner CS, Harnau L, Wittemann A (2009) 3D brownian diffusion of submicron-sized particle clusters. ACS Nano 3:3326–3334. https://doi.org/10.1021/nn900902b
28. Sheu HR, El-Aasser MS, Vanderhoff JW (1990) Uniform nonspherical latex particles as model interpenetrating polymer networks. J Polym Sci A Polym Chem 28:653–667. https://doi.org/10.1002/pola.1990.080280315
29. Park J-G, Forster JD, Dufresne ER (2009) Synthesis of colloidal particles with the symmetry of water molecules. Langmuir 25:8903–8906. https://doi.org/10.1021/la901969d